LIST OF PUBLICATIONS

1) K.Kaewyai, S. Choopun, M. Thepnurat, A.Gardchareon, S. Phadunghitidhada, , and D.Wongratanaphisan, "Preparation and characterization of copper oxide nanofibers by microwave-assisted thermal oxidation", Journal of Nanoelectronics and Optoelectronics 8 (2013) 472- 476. (IF = 0.4)

2) K. Kaewyai, S.Choopun, A. Gardchareon, P. Ruankham, S. Phadungdhitidhada, and D. Wongratanaphisana, "Effects of mixed-phase copper oxide nanofibers in ZnO dye-sensitized solar cells on efficiency enhancement" , Journal of Nanoscience and Nanotechnology, Accepted status . (IF =1.33)

3) K. Kaewyai, S.Choopun, A. Gardchareon, P. Ruankham, S. Phadungdhitidhada, and D. Wongratanaphisana, "CuO-Cu_2O nanocomposite layer for light-harvesting enhancement in ZnO dye-sensitized solar cells", Submitted to Materials Chemistry and Physics.

4) K. Kaewyai, S.Choopun, A. Gardchareon, P. Ruankham, S. Phadungdhitidhada, and D. Wongratanaphisana, "Mechanism and experimental evidence of rapid morphological variant of copper oxide nanostructures by microwave heating", Submitted to Nanoscale.

5) Karakade Kaewyai, Atcharawon Gardchareon, Supab Choopun , Suurachet Phadunghitidhada, Meechai Thepnurat and Duangmanee Wongratanaphisan, "Preparation of Nanocopper Oxides by Microwave and Characterization", Proceeding of Collaborative Conference on 3D & Materials Research (2013).

6) Karakade Kaewyai, Supab Choopun, Atcharawon Gardchareon, Surachet Phadunghitidhada,and DuangmaneeWongratanaphisan, "Synthesis and Characterization of Copper Oxide Nanofibers", Proceeding of International Conference on Nano/Molecular Medicine and Engineering (2013).

7) K. Kaewyai, A. Gardchareon, S. Choopun, S. Phadunghitidhada, P. Ruankham and D. Wongratanaphisan, “Screening copper oxide nanofibers as a barrier in ZnO dye-sensitized solar cells for efficiency enhancement” Proceeding of Eighth International Conference on Molecular Electronics and Bioelectronics (2015).

APPENDIX A

Characterizations of Copper Oxide Nanostructures Nanostructures

1. The TEM Analysis of Copper Oxide Nanoparticles by Camera-Constant Method

1.1 CuO nanoparticles

This method uses the camera constant ($L\lambda$) and diffraction pattern of the nanoparticle in spot pattern to identify the type and the structure of single crystal. The analysis is as follows:

- Measure the distance from a chosen spot (or spot center) to the 4 closer spots as shown in Figure A.1.
- Calculate d_{hkl} by using:

$$d_{hkl} = \frac{L\lambda}{r} \tag{A.1}$$

where d_{hkl} is the d-spacing, $L\lambda$ is the camera constant (20.2530 mmÅ) and r is the vector from measured distance. Thus,

$$d_1 = \frac{L\lambda}{r_1} = \frac{20.2530 \text{ mm}\,\text{Å}}{8 \text{ mm}} = 2.5316 \text{ Å}$$

$$d_2 = \frac{L\lambda}{r_2} = \frac{20.2530 \text{ mm}\,\text{Å}}{10.4 \text{ mm}} = 1.9474 \text{ Å}$$

$$d_3 = \frac{L\lambda}{r_3} = \frac{20.2530 \text{ mm}\,\text{Å}}{7.6 \text{ mm}} = 2.6648 \text{ Å}$$

$$d_4 = \frac{L\lambda}{r_4} = \frac{20.2530 \text{ mm}\,\text{Å}}{11.6 \text{ mm}} = 1.7459 \text{ Å}$$

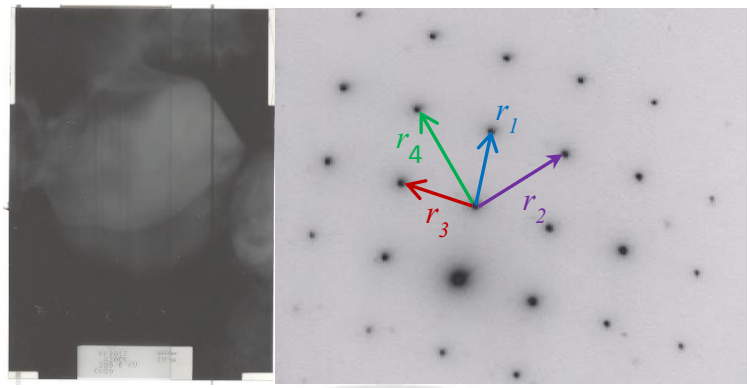

(a) (b)

Figure A.1 (a) TEM image of a copper oxide nanoparticle and (b) the diffraction pattern of the nanoparticle with r.

- To compare $d_1, d_2, d_3,$ and d_4 to d_{hkl} in the data base, this is shown in Figure A.2. From the data base, d_1, d_2, d_3 and d_4 are a plane of 002, $1\bar{1}2$, $\bar{1}10$ and $\bar{1}12$, respectively.

CuO_Base
CaRIne v3.0

dhkl	(hkl)	Sind?	Teta	Fs?	P	I%
5.058	(001)	1	8.76	4.00	2	100
4.619	(100)	1	9.60	0.00	2	0
3.733	(-101)	2	11.91	0.00	2	0
3.427	(010)	1	12.99	0.00	2	0
3.160	(101)	2	14.11	0.00	2	0
2.837	(0-11)	2	15.76	0.00	4	0
	(011)	2	15.76	0.00	4	0
2.752	(-110)	2	16.25	4.00	4	55
	(110)	2	16.25	4.00	4	55
2.529	(002)	4	17.73	4.00	2	23
2.524	(-111)	3	17.77	4.00	4	45
	(11-1)	3	17.77	4.00	4	45
2.391	(-102)	5	18.79	0.00	2	0
2.323	(1-11)	3	19.37	4.00	4	37
	(111)	3	19.37	4.00	4	37
2.309	(200)	4	19.48	4.00	2	18
2.246	(20-1)	5	20.06	4.00	2	17
2.078	(102)	5	21.76	0.00	2	0
2.035	(012)	5	22.24	0.00	4	0
	(0-12)	5	22.24	0.00	4	0
1.980	(201)	5	22.89	4.00	2	13
1.961	(-1-12)	6	23.13	4.00	4	25
	(-112)	6	23.13	4.00	4	25
1.915	(2-10)	5	23.72	0.00	4	0
	(210)	5	23.72	0.00	4	0
1.879	(-211)	6	24.21	0.00	4	0
	(21-1)	6	24.21	0.00	4	0
1.866	(-202)	8	24.38	4.00	2	11
1.777	(1-12)	6	25.69	4.00	4	20
	(112)	6	25.69	4.00	4	20
1.715	(2-11)	6	26.69	0.00	4	0
	(211)	6	26.69	0.00	4	0

Figure A.2 Data base of CuO to compare the d_{hkl}.

- The possible vectors are checked as shown in Figure A.3

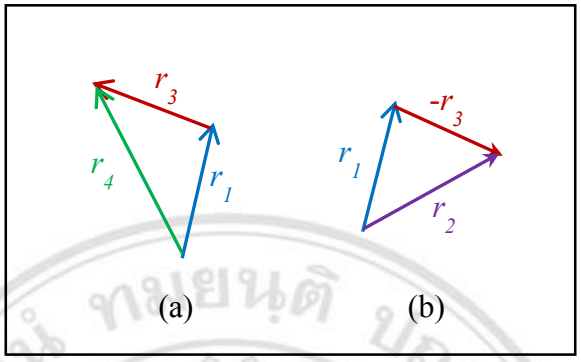

Figure A.3 Checked vectors for d_{hkl}.

$$\vec{r}_1 + \vec{r}_3 = \vec{r}_4$$
$$002 + \bar{1}10 = \bar{1}12$$

and

$$\vec{r}_1 + (-\vec{r}_3) = \vec{r}_2$$
$$002 + 1\bar{1}0 = 1\bar{1}2$$

- To find the direction of the electron beam incident by using right-hand rule of the cross vector, this is shown in Figure A.4. Any couple of vector is crossed in a clockwise direction and give same result of $[uvw]$.

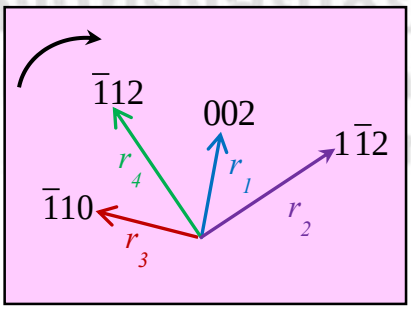

Figure A.4 Cross vectors for $[uvw]$.

$$\vec{r}_1 \times \vec{r}_2 \Rightarrow \begin{vmatrix} h & k & l \\ 0 & 0 & 2 \\ 1 & -1 & 2 \end{vmatrix} \Rightarrow [uvw] = [002]$$

$$\vec{r}_4 \times \vec{r}_1 \Rightarrow \begin{vmatrix} h & k & l \\ -1 & 1 & 2 \\ 0 & 0 & 2 \end{vmatrix} \Rightarrow [uvw] = [002]$$

$$\vec{r}_3 \times \vec{r}_4 \Rightarrow \begin{vmatrix} h & k & l \\ -1 & 1 & 0 \\ -1 & 1 & 2 \end{vmatrix} \Rightarrow [uvw] = [002]$$

$$\vec{r}_3 \times \vec{r}_1 \Rightarrow \begin{vmatrix} h & k & l \\ -1 & 1 & 0 \\ 0 & 0 & 2 \end{vmatrix} \Rightarrow [uvw] = [002]$$

Thus, $[uvw] = [002]$.

- To check for zone law this will present as, by follows;

$$hu + kv + lw = 0 \left(ZOLZ \right) \qquad \text{(A.2)}$$

where hkl is the Miller indices for planes in crystal (Bravais) lattices, and uvw is the Miller indices for the direction of electron beam incident or zone axis.

According to Equation (A.2),

$$(002) \cdot [uvw] = (002) \cdot [220] = 0$$
$$(1\bar{1}2) \cdot [uvw] = (1\bar{1}2) \cdot [220] = 0$$
$$(\bar{1}10) \cdot [uvw] = (\bar{1}10) \cdot [220] = 0$$
$$(\bar{1}12) \cdot [uvw] = (\bar{1}12) \cdot [220] = 0$$

The nanoparticle is a single crystal and its plans are 002, $1\bar{1}2$, $\bar{1}10$ and $\bar{1}12$, respectively. Moreover, the zone axis of the crystal is $[002]$. Therefore, the results correspond to the monoclinic structure of the CuO.

1.2 Cu_2O nanoparticles

The diffraction pattern of some nanoparticles showed in ring pattern, which can be identified type and structure by camera constant methods as follows:

- To find radius, measure the distance from a spot center to the diffraction spots as shown in Figure A.5.

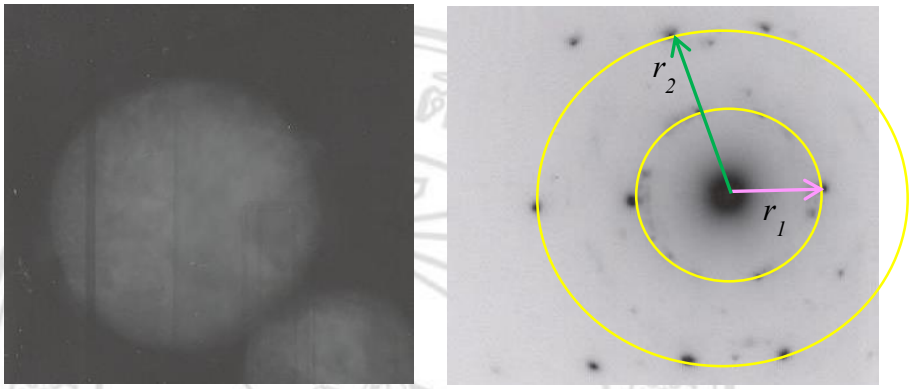

(a) (b)

Figure A.5 (a) TEM image of a copper oxide nanoparticle and (b) the diffraction pattern of the nanoparticle with r.

From the Figure A.5 (b), $r_1 = 9\ mm$ and $r_2 = 15\ mm$.

- Equation (A.1) is used to calculate d_{hkl} .Thus,

$$d_1 = \frac{L\lambda}{r_1} = \frac{20.2530\ \text{mm}\,\overset{0}{\text{A}}}{9\ \text{mm}} = 2.2503\ \overset{0}{\text{A}}$$

$$d_2 = \frac{L\lambda}{r_2} = \frac{20.2530\ \text{mm}\,\overset{0}{\text{A}}}{15\ \text{mm}} = 1.3502\ \overset{0}{\text{A}}$$

- Data base in program CaRIne v3.1 was used to compare d_1 and d_2. From the data base, the results correspond to Cu_2O structure.

2. The TEM Analysis of Copper Oxide Nanofibers

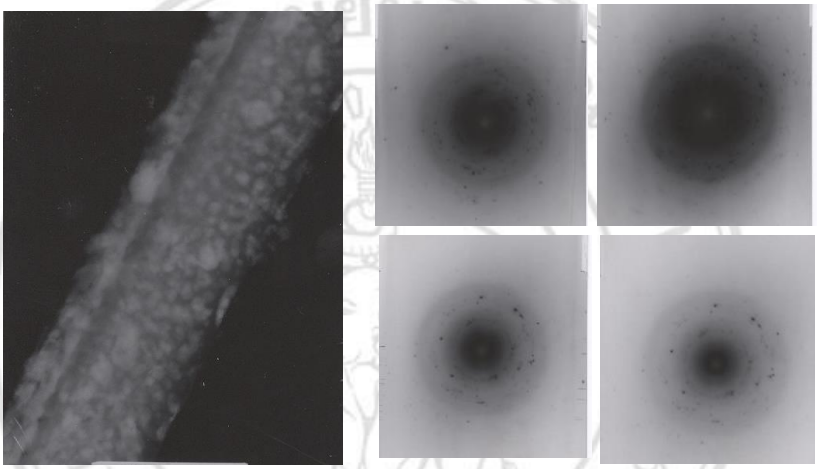

(a) (b)

Figure A.6 (a) A copper oxide nanofiber with white spots sticking on the fibers and (b) diffraction patterns of the white spots on the fiber.

The diffraction pattern of some spots sticking on the fibers showed in ring pattern, which can be identified type and structure by camera constant methods as follows:

- To find radius, measure the distance from a spot center to the diffraction spots as shown in Figure A.7.

- Equation (A.1) is used to calculate d_{hkl}. Thus,

Sample 1; $$d_1 = \frac{L\lambda}{r_1} = \frac{20.2530 \text{ mm}\,\text{Å}^0}{8.0 \text{ mm}} = 2.25316 \text{ Å}^0$$

$$d_2 = \frac{L\lambda}{r_2} = \frac{20.2530 \text{ mm}\,\text{Å}^0}{8.8 \text{ mm}} = 2.3014 \text{ Å}^0$$

$$d_3 = \frac{L\lambda}{r_3} = \frac{20.2530 \text{ mm } \overset{0}{\text{A}}}{10.7 \text{ mm}} = 1.8928 \overset{0}{\text{A}}$$

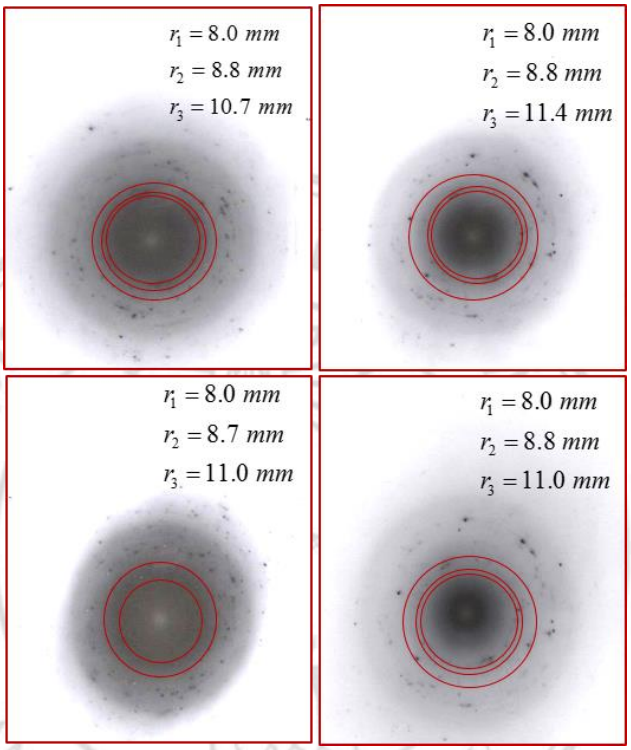

Figure A.7 Diffraction patterns of (a) the white spots in sample 1, (b) the white spots in sample 2, (c) the white spots in sample 3 and (d) the white spots in sample d.

Sample 2;
$$d_1 = \frac{L\lambda}{r_1} = \frac{20.2530 \text{ mm } \overset{0}{\text{A}}}{8.0 \text{ mm}} = 2.25316 \overset{0}{\text{A}}$$

$$d_2 = \frac{L\lambda}{r_2} = \frac{20.2530 \text{ mm } \overset{0}{\text{A}}}{8.8 \text{ mm}} = 2.3014 \overset{0}{\text{A}}$$

$$d_3 = \frac{L\lambda}{r_3} = \frac{20.2530 \text{ mm } \overset{0}{\text{A}}}{11.4 \text{ mm}} = 1.7765 \overset{0}{\text{A}}$$

Sample 3;
$$d_1 = \frac{L\lambda}{r_1} = \frac{20.2530 \text{ mm } \overset{0}{\text{A}}}{8.0 \text{ mm}} = 2.25316 \overset{0}{\text{A}}$$

$$d_2 = \frac{L\lambda}{r_2} = \frac{20.2530 \text{ mm}\,\text{Å}^0}{8.7 \text{ mm}} = 2.3279\ \text{Å}^0$$

$$d_3 = \frac{L\lambda}{r_3} = \frac{20.2530 \text{ mm}\,\text{Å}^0}{11.0 \text{ mm}} = 1.8441\ \text{Å}^0$$

Sample 4; $$d_1 = \frac{L\lambda}{r_1} = \frac{20.2530 \text{ mm}\,\text{Å}^0}{8.0 \text{ mm}} = 2.25316\ \text{Å}^0$$

$$d_2 = \frac{L\lambda}{r_2} = \frac{20.2530 \text{ mm}\,\text{Å}^0}{8.8 \text{ mm}} = 2.3014\ \text{Å}^0$$

$$d_3 = \frac{L\lambda}{r_3} = \frac{20.2530 \text{ mm}\,\text{Å}^0}{11.0 \text{ mm}} = 1.8441\ \text{Å}^0$$

Data base in program CaRIne v3.1 was used to compare d_1 and d_2. From the data base, d_1, d_2 and d_3 of each sample are presented in Table A.1 It is clearly shown that the results correspond to CuO structure.

Table A. 1 A comparison of the d_{hkl} from calculation with data base in program CaRIne v3.1.

Sample	Calculation of d_{hkl}	Data base of d_{hkl}			% error	
		CuO_Base center	Cu_2O_Body center	Cu_2O_Face center	CuO	Cu_2O
1	2.5316	2.529	2.342	2.342	0.61	8.09
	2.3014	2.322	2.342	2.342	0.89	1.73
	1.8928	1.878	1.912	1.912	0.79	1.00
2	2.5316	2.529	2.342	2.342	0.61	8.09
	2.3014	2.322	2.342	2.342	0.89	1.73
	1.7765	1.776	1.656	1.656	0.03	7.28

3	2.5136	2.529	2.342	2.342	0.61	8.09
	2.3278	2.322	2.342	2.342	0.25	1.54
	1.8411	1.866	1.912	1.912	1.33	3.71
4	2.5316	2.529	2.342	2.342	0.61	8.09
	2.3014	2.322	2.342	2.342	0.89	1.73
	1.8411	1.866	1.912	1.912	1.33	3.71

APPENDIX B

Deriving physics equations

1. The Penetration Depth of Conductor

As following Eq. (3.1) and Eq. (3.2), $d = \frac{1}{\alpha}$,

where α is the attenuation factor and can be represented as

$$\alpha = \omega\sqrt{\frac{\mu_0\mu'\varepsilon_0\varepsilon'}{2}}\sqrt{\left[1+\left(\varepsilon''_{eff}/\varepsilon'\right)^2\right]^{1/2}-1}.$$

For conductor being as high dielectric loss medium, $\varepsilon''_{polarization} = 0, \varepsilon''_{eff}/\varepsilon' >> 1$.

Thus,

$$\alpha = \sqrt{\frac{\omega^2 \mu_0 \mu' \varepsilon_0 \varepsilon'}{2}} \sqrt{\left[1 + \left(\frac{\varepsilon''_{eff}}{\varepsilon'}\right)^2\right]^{\frac{1}{2}}} \text{-1}$$

$$= \sqrt{\frac{\omega^2 \mu_0 \mu' \varepsilon_0 \varepsilon'}{2}} \sqrt{\left(\frac{\varepsilon''_{eff}}{\varepsilon'}\right)}$$

$$= \sqrt{\frac{\omega^2 \mu_0 \mu' \varepsilon_0 \varepsilon' \varepsilon''_{eff}}{2\varepsilon'}}$$

$$= \sqrt{\frac{\omega^2 \mu_0 \mu' \varepsilon_0 \varepsilon''_{eff}}{2}}$$

Therefore, $d = \frac{1}{\alpha} = \sqrt{\frac{\omega^2 \mu_0 \mu' \varepsilon_0 \varepsilon''_{eff}}{2}}$.

Because ε''_{eff} is the summation of losses from polarization and conduction,

$$\varepsilon''_{eff} = \varepsilon''_{polarization} + \varepsilon''_{conduction}$$

$$= \varepsilon''_{polarization} + \frac{\sigma}{\omega \varepsilon_0}$$

and for conductor $\varepsilon''_{polarization} = 0$.

Thus,

$$\varepsilon''_{eff} = \frac{\sigma}{\omega \varepsilon_0}$$

$$\sigma = \omega \varepsilon_0 \varepsilon''_{eff}$$

$$\sigma = \frac{1}{\rho}.$$

Therefore,

$$
\begin{aligned}
d = \frac{1}{\alpha} &= \sqrt{\frac{2}{\omega^2 \mu_0 \mu' \varepsilon_0 \varepsilon''_{eff}}} \\
&= \sqrt{\frac{2}{\omega \mu_0 \mu' \left(\omega \varepsilon_0 \varepsilon''_{eff}\right)}} \\
&= \sqrt{\frac{2}{\omega \mu_0 \mu' \sigma}} \\
&= \sqrt{\frac{2}{2\pi f \mu_0 \mu' \sigma}} \\
&= \sqrt{\frac{1}{\pi f \mu_0 \mu' \sigma}} \\
&= \sqrt{\frac{\rho}{\pi f \mu_0 \mu'}},
\end{aligned}
$$

assume $\mu' = 1$, $d = \sqrt{\frac{\rho}{\pi f \mu_0}}$ or $d = \sqrt{\frac{1}{\sigma \pi f \mu_0}}$.

2. Gibbs Equation with Nucleation

Following Gibbs equation in Eq. (3.8), at critical point $(d\Delta G / dr) = 0$, so

$$
\begin{aligned}
\frac{d}{dr}\Delta G &= \frac{d}{dr}\left(4\pi r^2 \gamma\right) + \frac{d}{dr}\left(\frac{4}{3}\pi r^3 \Delta G_V\right) \\
0 &= 8\pi r\gamma + 3\left(\frac{4}{3}\right)\pi r^2 \Delta G_V \\
0 &= 8\pi r\gamma + 4\pi r^2 \Delta G_V \\
-4\pi r^2 \Delta G_V &= 8\pi r\gamma \\
-4\pi r^2 \Delta G_V &= 8\pi r\gamma \\
-r\Delta G_V &= 2\gamma \\
r &= -\frac{2\gamma}{\Delta G_V}.
\end{aligned}
$$

At critical radius, $r = r_c$, the total free energy of the system, ΔG, is written as follows:

$$\begin{aligned}\Delta G &= 4\pi\left(-\frac{2\gamma}{\Delta G_V}\right)^2\gamma + \frac{4}{3}\pi\Delta G_V\left(-\frac{2\gamma}{\Delta G_V}\right)^3 \\ &= \frac{16\pi\gamma^3}{\Delta G_V{}^2} - \frac{32\pi\gamma^3}{3\Delta G_V{}^2} \\ &= \frac{48-32}{3}\left(\frac{\pi\gamma^3}{\Delta G_V{}^2}\right) \\ &= \frac{16\pi\gamma^3}{3\Delta G_V{}^2}.\end{aligned}$$

Due to the total free energy of the system at the critical radius, r_c, shows the maximum energy barrier of height, so $\Delta G = \Delta G^* = \frac{16\pi\gamma^3}{3\Delta G_V{}^2}$.

However, free energy change per unit volume of solid from the liquid, ΔG_V, depends on pressure of supersaturation , S , as shown in Eq. (3.10),

$$\Delta G_V = \frac{-k_B T}{\Omega}\ln(1+S).$$

Therefore, $\Delta G^* = \frac{16\pi\gamma^3}{3\Delta\left(\frac{-k_B T}{\Omega}\ln(1+S)\right)^2}$ and this clearly shows that the maximum energy barrier, ΔG^*, decreases with increasing of supersaturation , S .

APPENDIX C

The Physics Definition

1. Polarization Mechanisms

Table C.1 Mechanisms of different polarizations [91].

Kinds of polarization	No E field (E=0) ← Local E field ← (E≠0)	Mechanisms
Electronic		Electrons in an external electric field are shifted from equilibrium with respect to the positive nuclei and resulted in an induced dipole moment.
Orientation		The randomly oriented dipole moments respond to external electric field, try to align these asymmetric polar molecules leading to permanent dipoles parallel to the field.
Ionic	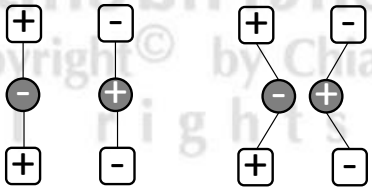	The positive and negative changes in crystals are displaced from their equilibrium position under external electric field resulting in the net dipole moment is non zero.
Interfacial	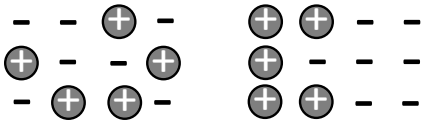	Under an external electric field, the more charges are displaced and accumulated at barrier resulting in interfacial polarization.

Polarization generally just means “orientation.” Polarization occurs from some kind of asymmetry in the interaction between spin and electromagnetic fields or matter. For electromagnetic waves, the vectors are the electric and magnetic fields, and the light’s polarization direction is by convention along the direction of the electric field. The illustrates of four kinds of polarization mechanism, electronic polarization, orientation polarization, ionic polarization, and interfacial polarization, and their mechanisms are shown in Table C.1.

2. Dielectric loss

When an external electric field is applied to a dielectric material, some amount of electrical energy is absorbed by the dielectric material and is wasted in the form of heat. This loss is known as dielectric loss. A dielectric loss occurs from movement or rotation of atoms or molecules in an alternating electric field.

For microwave engineering, a loss material can be represented by relative dielectric constant, ε', and dissipation factor or loss tangent, $\tan\delta$, as the following equation [91]

$$\tan\delta = \frac{\varepsilon''_{eff}}{\varepsilon'},$$

where δ is a phase lag, which occurred from dipolar reorientation of dielectric material in alternating electric field of microwave, ε''_{eff} is the effective relative dielectric loss factor (a measure of the efficiency of converting microwave energy into heat), and ε' is relative dielectric constant (a measure of polarization of a molecule in an electric field).

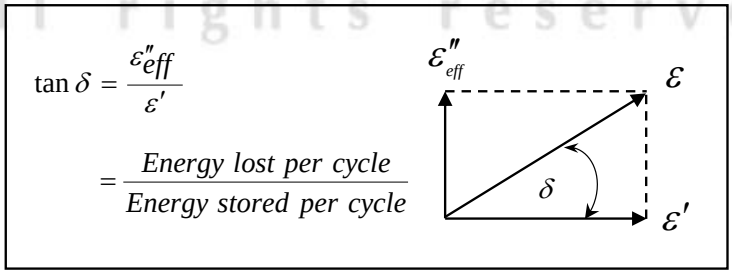

Figure C.1 Loss tangent vector diagram.

The loss tangent vector diagram is shown in Figure C.1 ($\mathcal{E}$ is relative permittivity). For very low loss materials, since $\tan\delta \approx \delta$, the loss tangent can be expressed in angle units, milliradians or microradians. Therefore, the loss power of microwave per surface area in a material due to dielectric loss, $P_{dielectric\ loss}$, as following [91]

$$P_{dielectric\ loss} = \omega\varepsilon_0\varepsilon' \tan\delta \left|E_0\right|^2 .$$

CURRICULUM VITAE

Author's Name	Miss Karakade Kaewyai	
Date/Year of Birth	September 25, 1978	
Place of Birth	Krabi Province, Thailand	
Occupation	2005–2006	Lecturer at King Mongkut's Institute of Technology Ladkrabang, Chumphon Campus, Thailand
	2006–2012	Lecturer at Thaksin University, Phattalung Campus, Thailand
Office address	Physics Department, Faculty of Science, Thaksin University, Phattalung, Thailand 93110	
Education	1997–2000	B.Sc. (Physics) Prince of Songkla University, Pattani Campus, Thailand
	2001–2004	M. Sc. (Applied Physics), Chiang Mai University, Thailand
	2012–2016	Ph. D. (Applied Physics), Chiang Mai University, Thailand
Scholarship	2012–2015	Ministry of Science and Technology (Thailand)
	2015	The Graduate School of Chiang Mai University

Publications

1. K.Kaewyai, S. Choopun, M. Thepnurat, A.Gardchareon, S. Phadunghitidhada, , and D.Wongratanaphisan, "Preparation and characterization of copper oxide nanofibers by microwave-assisted thermal oxidation", Journal of Nanoelectronics and Optoelectronics 8 (2013) 472- 476.

2. K. Kaewyai, S.Choopun, A. Gardchareon, P. Ruankham, S. Phadungdhitidhada, and D. Wongratanaphisana, “Effects of mixed-phase copper oxide nanofibers in ZnO dye-sensitized solar cells on efficiency enhancement” , Journal of Nanoscience and Nanotechnology, Accepted status.

3. K. Kaewyai, S.Choopun, A. Gardchareon, P. Ruankham, S. Phadungdhitidhada, and D. Wongratanaphisana, “CuO-Cu_2O nanocomposite layer for light-harvesting enhancement in ZnO dye-sensitized solar cells”, Submitted to Materials Chemistry and Physics.

4. K. Kaewyai, S.Choopun, A. Gardchareon, P. Ruankham, S. Phadungdhitidhada, and D. Wongratanaphisana, “Mechanism and experimental evidence of rapid morphological variant of copper oxide nanostructures by microwave heating”, Submitted to Nanoscale.

Conferences

1. Karakade Kaewyai, Atcharawon Gardchareon, and Duangmanee Wongratanaphisan, “Synthesis and Characterization of Nanocopper Oxides”, International Workshop on Conference of Physics and Material Engineering (2013).

2. Karakade Kaewyai, Atcharawon Gardchareon, Supab Choopun , Suurachet Phadunghitidhada, Meechai Thepnurat and Duangmanee Wongratanaphisan, “Preparation of Nanocopper Oxides by Microwave and Characterization”, Collaborative Conference on 3D & Materials Research (2013).

3. Karakade Kaewyai, Supab Choopun, Atcharawon Gardchareon, Surachet Phadunghitidhada,and Duangmanee Wongratanaphisan, “Synthesis and Characterization of

Copper Oxide Nanofibers", International Conference on Nano/Molecular Medicine and Engineering (2013).

4. Chawalit Bhoomanee, Karakade Kaewyai, Supab Choopun, Sutthipoj Sutthana, Sornchai Tananchai, and Duangmanee Wongratanaphisan, "Annealing Effect of AZO Multilayer Thin Films", International Conference on Nano/Molecular Medicine and Engineering (2013).

5. K. Kaewyai, A. Gardchareon, S. Choopun, S. Phadunghitidhada, P. Ruankham and D. Wongratanaphisan, "Screening copper oxide nanofibers as a barrier in ZnO dye-sensitized solar cells for efficiency enhancement" Eighth International Conference on Molecular Electronics and Bioelectronics (2015).

Seminar/ Experience/ Training

1. Graduate Students Seminar in Technical of Research Publication: Regulations on Graduate Education 2554, on 12th December, 2012, time 8.30 - 13.00, Chiang Mai University

2. Siam Physics Congress 2013, during 21st–23th March, 2013 at Chiangmai Grandview Convention Center, Chiang Mai

3. Nanoscience and Nanotechnology Annual Seminar 2012, on 2nd April, 2013, time 9.00-15.30, Chiang Mai University.

4. English Training by Language Institute: Funding from Department of Physics and Materials Science, during 1st – 24th April, 2013 at Language Institute, Chiang Mai University.

5. Training of Oral Presentation in English: Funding from Graduate School, during 9th – 11th September, 2013 at Graduate School, Chiang Mai University.